U.S. AIR FORCE

Determining Bulk Aerosol Absorption from Off-Axis Backscattering using Rayleigh Beacon Laser Pulses

Julie C. Grossnickle, Capt, USAF
AFIT/ENP

Outline

- Introduction
- Methodology
- Results
- Conclusions
- References

Introduction

- Motivation
  - The extent of aerosol effects are not fully understood. The quantification and measurement of aerosol absorption properties remains a challenge.
  - As HELs become more prevalent in defense operations, the ability to quantify laser performance degradation from aerosols becomes increasingly more important.
  - Understanding aerosol optical properties from laser energy propagation can have implications for the climate change research community.
- Objectives
  - Test the hypothesis that measured off-axis backscatter from high-energy lasers can be used to determine bulk aerosol absorption.
  - To develop a technique that can be applied in both high-energy laser applications and within the atmospheric science communities.

Methodology

The AFIT of Today is the Air Force of Tomorrow.

➢ Field Measurements

- Laser Images

1. Visible off-axis laser images of Rayleigh beacon pulse laser at John Bryan Observatory in Yellow Springs OH, captured using G9 Canon camera.

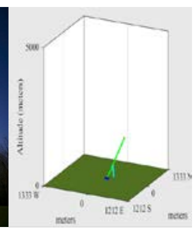

2. Examined brightness and intensity changes in digital pixel values along the length of the beam

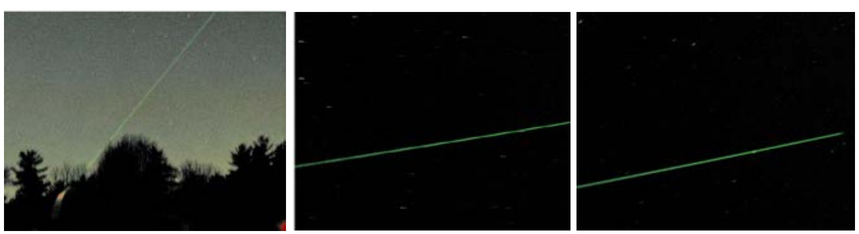

- Aerosol Data:

1. MAGIC200 Condensation Particle Counter
2. Scanning Mobility Particle Sizer

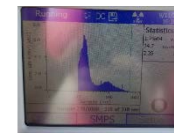

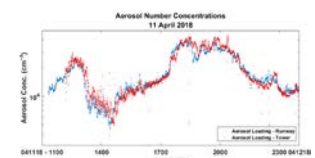

3. Global Aerosol Data Set (GADS)

➢ Climatological database: describes seasonal surface aerosol number concentrations, size distributions, and optical properties for 10 aerosol component types

SEASON	INSOLUBLE (cm^{-1})	SOOT (cm^{-1})	WATER-SOLUBLE (cm^{-1})	TOTAL # CONCENTRATION
Winter	0.5	15,000	11,000	26,000.5
Summer	0.5	15,000	13,200	28,000.5

Methodology

- Predicted Off-Axis Scattered Irradiance and the Phase Function
  - High Energy Laser End-to-End Operational Simulation (HELEEOS)
    - Off-axis algorithm: calculates laser energy in any off-axis direction, taking into account phase angle, particle cross section and number concentration, and distance to observation point.

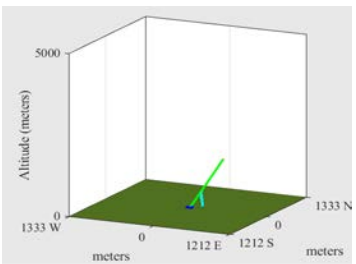

$$I_{SCA} = \sum_{i=1}^{100} \frac{P(\Theta)_i \beta_{SCAi} I_{Oi}}{4\pi R_i^2} dv_i$$

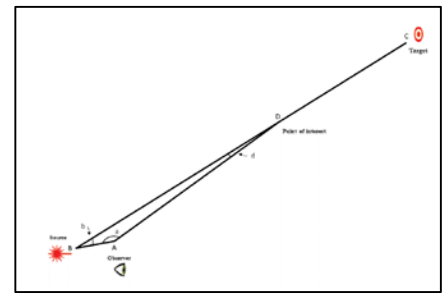

  - Laser Environmental Effects Definition and Reference (LEEDR)
    - Calculates the relative amount of scattered irradiance from aerosols (Mie theory), and from gas molecules (Rayleigh theory) at each phase function angle.

$$\frac{\beta_s}{4\pi} \int_{4\pi} p(\widehat{\Omega}', \widehat{\Omega}) I(\widehat{\Omega}') d\omega' \, ds$$

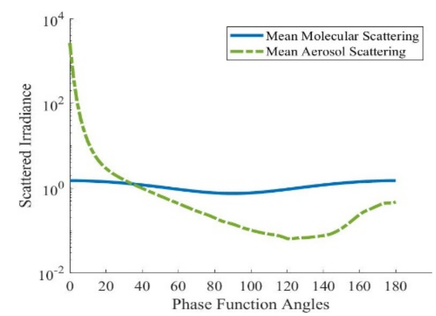

Results

➢ Laser Images

- Image of the upper portion of the beam. Pixel index and location are plotted to show the increase in brightness values along the length of the beam.

- This shows an increase in scattered irradiance at larger phase angles.

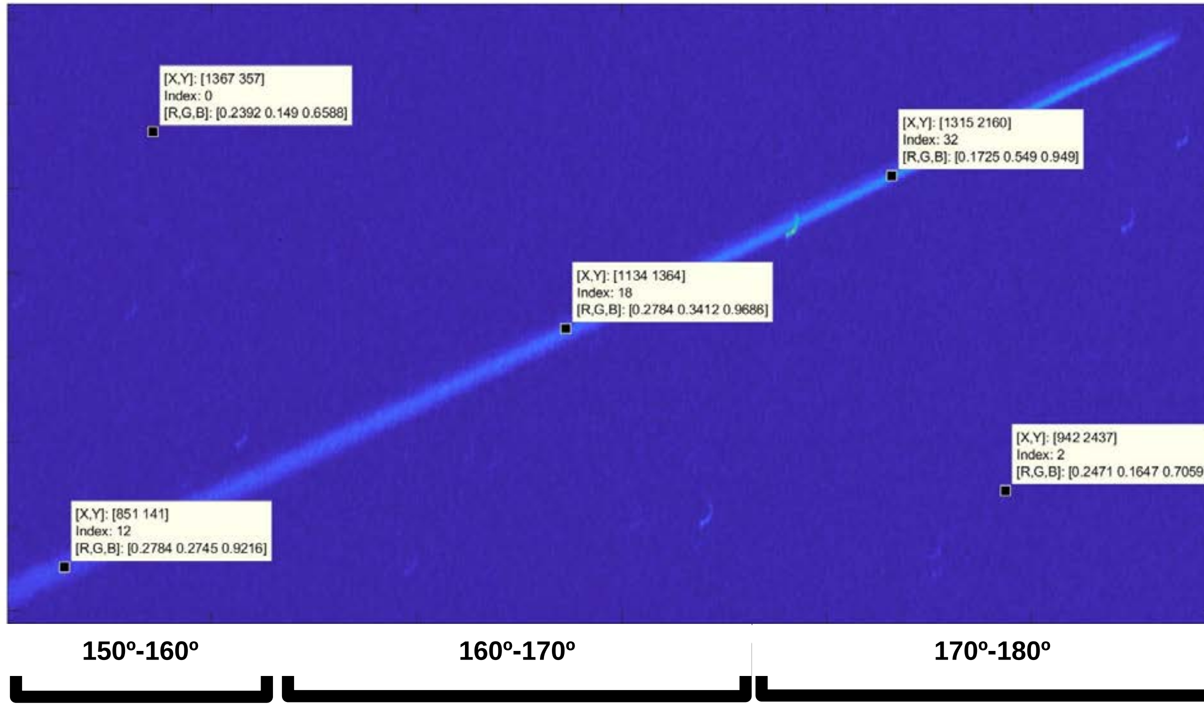

Results

- Predicted Scattered Irradiance at Off-Axis Observation Location
- Using a ±0.4 angular view, observer irradiance are computed for several points along the beam.

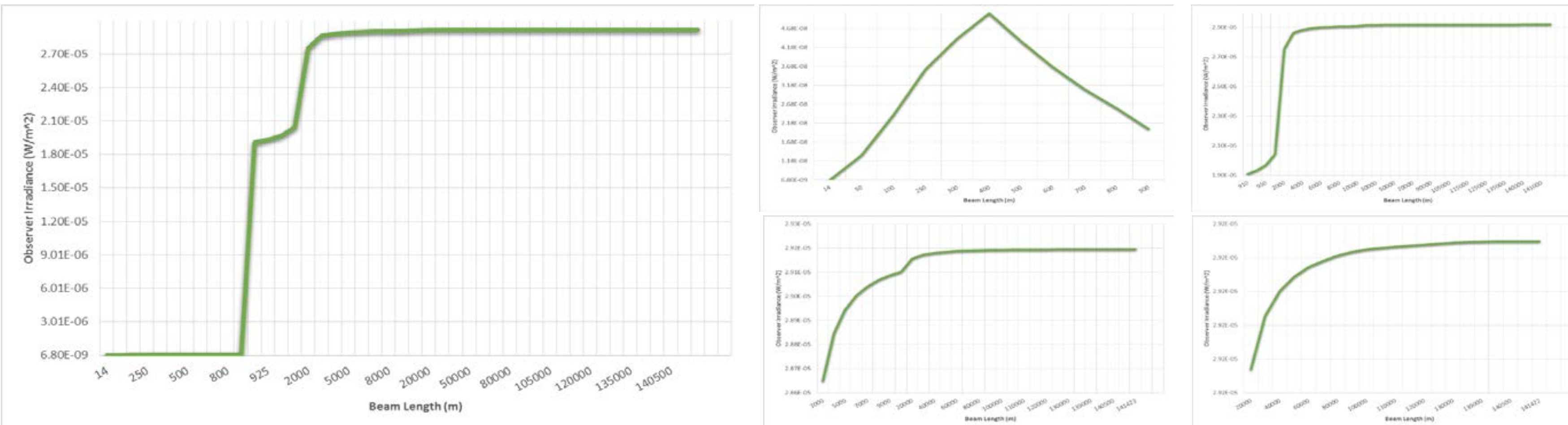

- The model predicts an increase in irradiance at larger phase angles, which are backward scatter angles. Larger image on the left is the entire beam length, while the small images on the right are zoomed in plots.
- Top middle reveals that the bottom most 500 m of the beam, has an increase in scattered irradiance at the observation location, followed by a steady decrease through the next 500 m.
- Top right and bottom middle show a rapid increase followed by a slow and steady increase. However, zooming in on the tail end of the laser beam, from approximately 20,000 m to 141,500 m, the plot shows a similar pattern of sharp increase, albeit at a smaller magnitude.
- The last 50,000 m of the beam reveals a very small increase in observer irradiance. However, at very small increments of off-axis angles, a camera lens would be viewing the same length of the beam.

Results

➢ Phase Function: varying imaginary component of CIR

- Multiple LEEDR-derived predicted phase function profiles. The black solid line represents molecular (Rayleigh) scattering, while the blue and green lines are the different aerosol scattering (Mie) phase functions resulting from various imaginary index values
- To capture full spectrum of common imaginary index values seen in local aerosol components the following values are used: 0.001i, 0.006i (GADS), 0.010i, 0.050i, 0.100i, 0.400i (soot).

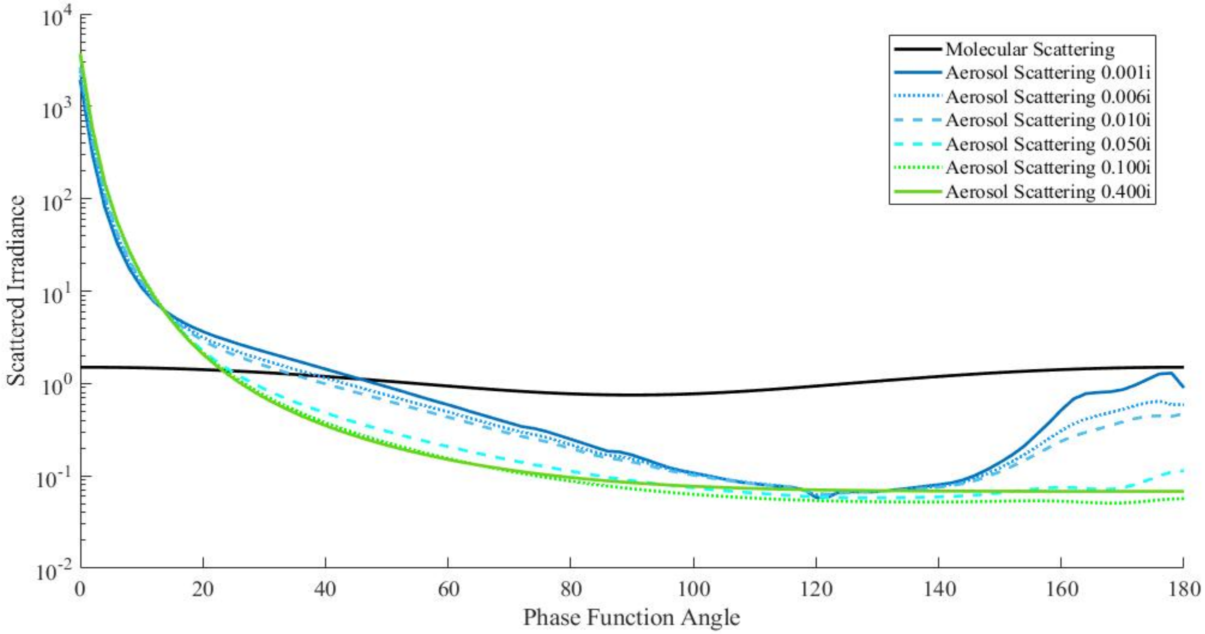

Conclusions

- Varying absorption properties (CIR) changes the shape of the phase function, notably at backward phase angles.

- Backscattered portion of scattering phase function offers the most information about aerosol optical properties for off-axis laser energy analysis
  - Laser images show additional brightness as approach 170-180 scattering angles
  - Backscattered imagery suggests bulk aerosol absorption values no greater than 0.05 at 527 nm

References

1. Andrews, Elisabeth, P.J. Sheridan, J.A. Ogren, D.H. Hageman, A. Jefferson, J. Wendell, A. Alastuey, L. Alados-Arboledas, M. Bergin, M. Ealo, A.G. Hallar, A. Hoffer, A. Hoffer, I. Kalapv, M. Keywood, J. Kim, S. Kim, F. Kolonjari, C. Labuschagne, N. Lin, A. Macdonald, O.L. Mayol-Bracero, I.B. McCubbin, M. Pandolfi, F. Reisen, S. Sharma, J.P. Sherman, M. Sorribas, and J. Sun. "Overview of the NOAA/ESRL Federated Aerosol Network," *Bull. Amer. Meteor. Soc.*, 100: 123-135 (January 2019).
2. Belton, S.L. The Simulation of Off-Axis Laser Propagation Using HELEEOS. MS Thesis, AFIT /GSS/ENP/06-01. Graduate School of Engineering and Management, Air Force Institute of Technology (AETC), Wright-Patterson AFB OH, March 2006.
3. Bergstrom R.W., P. Pilewskie, P.B. Russell, J. Redemann, T.C. Bond, P.K. Quinn, et al. "Spectral absorption properties of atmospheric aerosols," *Atmos. Chem. Phys*., 7(23), 5937-43 (2007).
4. Bond T.C., T.L. Anderson, and D. Campbell. "Calibration and Intercomparison of Filter-Based Measurements of Visible Light Absorption by Aerosols," *Aerosol Science & Technology,* 30(6), 582-600 (2010).
5. Burley J.L., S.T. Fiorino, B.J. Elmore, J.E. Schmidt. "A Fast Two-Stream-Like Multiple-Scattering Method for Atmospheric Characterization and Radiative Transfer," *J. Appl. Meteol. Climatol*., 56: 3049-3063 (August 2017).
6. Fiorino, S.T., J.A. Deibel, P.M. Grice, M.H. Novak, J. Spinoza, L. Owens, and S. Ganti. "A technique to measure optical properties of brownout clouds for modeling terahertz propagation." *Applied Optics*, 51: 3605-3613 (2012).
7. Fiorino, S.T., R.M. Randall, R.J. Bartell, J.D. Haiducek, M.F. Spencer, S.J. Cusumano. "Field measurements and comparisons to simulations of high energy laser propagation and off-axis scatter," *Proc. SPIE 7814, Free-Space Laser Communications X.* 78140P: 1-11 (August 2010).
8. Haiducek, John*. Experimental Validation Techniques for the HELEEOS Off-Axis Laser Propagation Model*. MS Thesis, AFIT/GE/ENP/10-M02. Graduate School of Engineering and Management, Air Force Institute of Technology (AETC), Wright-Patterson AFB OH, March 2010.
9. Hess, M., P. Koepke, and I. Schult. "Optical Properties of Aerosol and Clouds: The Software Package OPAC," Bull. Amer. Meteor. Soc., 79, No. 5: 831-844 (May 1998).
10. Koepke, Peter, M. Hess, I. Schult, and E.P. Shettle. *Global Aerosol Data Set: Report No. 243*. Hamburg Germany, Max-Planck-Institut fur Meteorologie, September 1997.
11. Liou, K.N. *An Introduction to Atmospheric Radiation* (2nd Edition). Academic Press, 2002.
12. Moosmuller, H., R.K. Chakrabarty, and W.P. Arnott. "Aerosol light absorption and its measurement: A review," *J. Quantitative Spectroscopy & Radiative Transfer*, 110: 844–878 (2009).
13. Petty, G.W. *A First Course in Atmospheric Radiation* (2nd Edition). Madison, WI: Sundog Publishing, 2006.
14. Perram, G.P., S.J. Cusumano, R.L. Hengehold, and S.T. Fiorino. *Introduction to Laser Weapon Systems*. Albuquerque, NM: Directed Energy Professional Society, 2010.
15. Samset B.H., C.W. Stern, E. Andrews, R.A. Kahn, G. Mire, M. Schulz, and G.L. Schuster. "Aerosol Absorption: Progress towards Global and Regional Constraints," *Current Climate Change Reports*, 4:65-83 (June 2018).

AMERICAN METEOROLOGICAL SOCIETY

100th Annual Meeting 12 - 16 January 2020

AMS 100
ADVANCING SCIENCE SERVING SOCIETY

Air Force Institute of Technology
Center for Directed Energy
Wright-Patterson AFB, Ohio

Determining Bulk Aerosol Absorption from Off-Axis Backscattering using Rayleigh Beacon Laser Pulses

J. C. Grossnickle[1], S. T. Fiorino[1], K. J. Keefer[1,2], H. R. Tseng[1], and R. C. Tournay[1]
AFIT Department of Engineering Physics
Julie.Grossnickle@afit.edu Steven.Fiorino@afit.edu Kevin.Keefer.ctr@afit.edu
Hsien-Liang.Tseng@afit.edu Robert.Tournay@afit.edu

Aerosol absorption and scattering can play a key role in degraded high energy laser performance in the form of thermal blooming and beam attenuation. Aerosol absorption properties are not completely understood and thus affects how we are able to quantify expected high energy laser weapon performance. The Air Force Institute of Technology Center for Directed Energy (AFIT CDE) developed both Laser Environmental Effects Definition and Reference (LEEDR) and the High Energy Laser End-to-End Operational Simulation (HELEEOS) codes to characterize atmospheric radiative transfer effects and evaluate expected directed energy weapon system performance. These packages enable modeling total irradiance at given off-axis locations through an off-axis scattering algorithm, which uses scattering phase functions to predict the amount of radiation scattered from the beam toward a particular observation location. The phase function shapes from off-axis high energy laser irradiance measurements taken at several different angles are compared to the predicted scattering phase function shapes. Laser energy measurements were conducted using a side telescope and ultrafast laser, located at John Bryan Observatory (JBO) in Yellow Springs, Ohio. The off-axis irradiance was measured using a Mini-SWIR JSX snapshot camera, calibrated to capture scattered irradiance in the visible spectrum. Aerosol characterization information was gathered using a Condensation Particle Counter (CPC), a Scanning Mobility particle Sizer (SMPS), and a Continuous Light Absorption Photometer (CLAP). The differences in the measured versus predicted phase function shapes elucidate bulk aerosol absorption properties.

Motivation:

- The extent of aerosol effects are not fully understood. The quantification and measurement of aerosol absorption properties remains a challenge.
- As HELs become more prevalent in defense operations, the ability to quantify laser performance degradation from aerosols becomes increasingly more important.
- Understanding aerosol optical properties from laser energy propagation can have implications for the climate change research community.

Methodology

Experiment Set-Up:

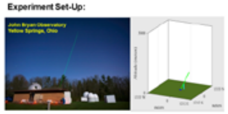

HELEEOS GUI allows for the user to select a specific point along the beam and set an angular observer field of view to retrieve scattered irradiance values received at the observer point from that particular section of the beam. By selecting various points along the length of the beam, can see how scattering changes along the beam.

Numerical Modeling Packages:

HELEEOS LEEDR

HELEEOS Off-Axis Calculations:
The scattering phase function is used to calculate how much laser energy is scattered in any off-axis direction. Taking into account phase angle, both scattering cross sections and number concentrations of particles, and the distance between the receiver and the beam, HELEEOS splits the beam into 1,000 different segments to calculate and sum scattered intensity using Mie scattering theory equations.

$$I_{SCA} = \sum_{i=1}^{100} \frac{P(\Theta)_i \beta_{SCA_i} I_{O_i}}{4\pi R_i^2} dv_i$$

Global Aerosol Data Set (GADS)

- Climatological database – describes surface aerosol number concentrations, size distributions, and optical properties for 10 constituents
- Seasonal variations are defined as the following:
  - Winter: September-February
  - Summer: March-August

SEASON	INSOLUBLE (cm^{-3})	SOOT (cm^{-3})	WATER-SOLUBLE (cm^{-3})	TOTAL # CONCENTRATION
Winter	0.5	15,000	11,000	26,000.5
Summer	0.5	15,000	13,200	28,000.5

GADS number concentrations per constituent for the Dayton, Ohio region

LEEDR-calculated phase function at 527 nm wavelength

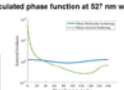

Raw Laser Images:

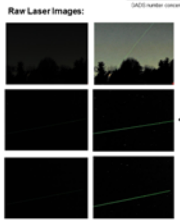

Figure 3. Image Processing Tool. Brightness and intensity changes in the pixel values along the beam path are used to analyze against HELEEOS-calculated irradiance values.

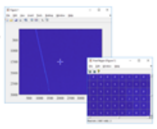

Figure 2. Off-Axis laser images captured with a G9 Canon camera. The left set of images are raw images of three different sections of the beam (bottom, middle, top). The right set of images are processed using a contrast enhancement (twice inverted and de-hazed) to make the laser beam easier to view.

Figure 4. Experiment setup with triangle shown between observer, source, and point of interest along the laser beam path. Geometry relevant to relate pixels to physical location.

Aerosol Measurements

- Aerosol characterization data (particle counts, size distributions, raw absorption) collected at JBO using:
  - MAGIC200 Condensation Particle Counter (CPC)
  - Scanning Mobility particle Sizer (SMPS)
  - Continuous Light Absorption Photometer (CLAP)

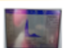

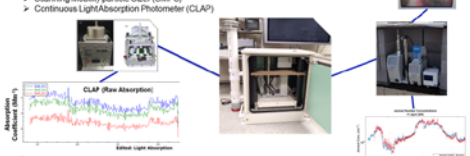

Raw absorption data collection was made possible by the NOAA Global Monitoring Division, specifically Patrick Sheridan and Betsy Andrews for providing the CLAP device.

Results

Analyzed Laser Images

Figure 5. Processed Images with index and pixel locations plotted throughout the image. Image is displayed with green channel highlighted in order to view the brightness values along the beam. Approximate backscattering angles are identified along the bottom of the image. Brightness values increase along the length of the beam, indicating that larger sections of the beam are being observed, and thus larger scattering values.

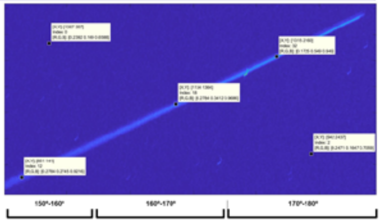

Scattered Irradiance at Off-Axis Observation Location

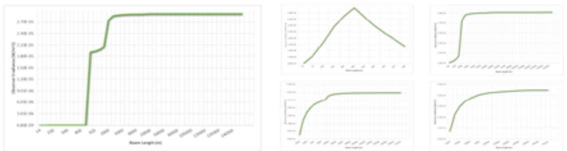

Figure 6. HELEEOS-calculated irradiance scattered from each section of the beam to the off-axis observation point. Demonstrates the change in scattered irradiance along the beam path, and that there is an increase in scattered irradiance at backscattering angles.

Scattering Phase Functions: varying imaginary component of CIR

Figure 7. LEEDR-calculated molecular (black) and aerosol (blue and green) scattering phase function profiles. Aerosol phase functions were computed with various imaginary index of refraction values, highlighting the changes in shape of the phase function with a pronounced difference at backscattering angles.

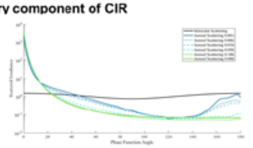

Conclusions:

- Varying absorption properties (CIR) changes the shape of the phase function, notably at backward phase angles.
- Backscattered portion of scattering phase function offers the most information about aerosol optical properties for off-axis laser energy analysis
  - Laser images show additional brightness as approach 170-180 scattering angles
  - Backscattered imagery suggests bulk aerosol absorption values no greater than 0.05 at 527 nm

Future Research:

- Use a calibrated camera in order to quantitatively capture scattered irradiance.
- Expand aerosol absorption research by applying thermal blooming displacement and distortion impacts on on-axis HEL spot measurements.

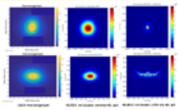

A special thanks to the DoD Joint Directed Energy Transition Office for funding support

[1]Air Force Institute of Technology
[2]Applied Research Solutions, Inc.